Available online at www.sciencedirect.com
SCIENCE DIRECT®
Physica C 425 (2005) 44–51
PHYSICA C
www.elsevier.com/locate/physc

High T_c superconductor re-entrant cavity filter structures

Himanshu Pandit [a], Donglu Shi [b,*], N. Hari Babu [c], X. Chaud [d], D.A. Cardwell [c], P. He [b], D. Isfort [d,e], Robert Tournier [e], David Mast [f], Altan M. Ferendeci [a]

[a] Department of Electrical and Computer Engineering and Computer Science, University of Cincinnati, Cincinnati, OH 45221, USA
[b] Department of Chemical and Materials Engineering, University of Cincinnati, Cincinnati, OH 45221, USA
[c] IRC in Superconductivity, University of Cambridge, Cambridge, UK
[d] Consortium de Recherches pour l'Emergence de Technologies Avancées, CNRS, BP 166, F-38042 Grenoble Cedex 9, France
[e] Laboratorie de Christallograpphie, CNRS, BP 166, F-38042 Grenoble Cedex 9, France
[f] Department of Physics, University of Cincinnati, Cincinnati, OH 45221, USA

Received 1 November 2004

Abstract

Microwave cavity filters are widely used in high frequency communication systems for high quality factor signal filtering. However, their large size makes it inconvenient for them to be used at lower operating frequencies especially in the 1–4 GHz frequency range of most of the present day commercial wireless applications. In order to improve their performance and to reduce their overall size, superconducting cavity filters were designed and simulated. Cylindrical and re-entrant cavity filters were fabricated, using seeded melt grown yttrium barium copper oxide high temperature superconductors. The resonant characteristics of these filters were measured, verifying the concept that small, high Q, cavity filters can be made for wireless applications.

1. Introduction

Frequency selective filters are one of the most crucial components in any communication system where the quality of the signal, voice or data, is highly dependent on the selectivity of the filter employed [1]. As the data rates in communication systems are increasing exponentially, the need for precise and highly accurate filters is also increasing. Researchers are periodically coming up with better and more efficient designs, making filter design a very competitive field. The filters used in different systems vary extensively depending on the system application. Some of the important characteristics to consider in selecting a filter are size, low insertion loss, high selectivity, bandwidth

* Corresponding author. Fax: +1 5113 556 2569.
E-mail address: shid@email.uc.edu (D. Shi).

0921-4534/$ - see front matter © 2005 Elsevier B.V. All rights reserved.
doi:10.1016/j.physc.2005.05.010

and noise margin [2,3]. In addition, the entire communication system and its associated components may present several constraints which may prevent a unique optimal design solution. Hence the choice of a filter is always a trade-off between filter characteristics and system constraints.

With the advances in integrated circuits development, planar transmission line filters of very small size can be fabricated and used in most applications. Despite the availability of these smaller sized filters, bulk cavity filters provide higher quality factor, or Q, which are several times higher than other filter types. The sharper characteristics also reduce the interference from neighbouring channels. Thus by employing a high quality filter, the requirement for extensive signal processing to eliminate noise can be reduced greatly.

Cavity filters are employed in applications where the size of the filter is not a significant constraint and the system operates over a narrow frequency range. In this case the selectivity of the filter is very important. Typically, cavity resonator filters find applications in high frequency wireless communication systems, satellite transmission systems and radars, where the quality of the signal is of paramount importance and size is largely irrelevant [1].

Even though the cavity resonators can provide high quality filtering, the major limitation of cavity filters is their bulky size in the range of frequencies in which most wireless applications operate. Most present day wireless systems cover the frequency range of 800 MHz to 5 GHz. For a cavity resonator to be used at 2 GHz, its radius is typically around 57 mm. Hence the use of these filters is limited to applications where space is not a constraint, while quality of filtering is of great importance. The aim of this research is to address the size limitations associated with conventional cavity filters, and thus to enhance their applications potential in state of the art communication systems.

Filters of high selectivity and high quality factors have been designed and implemented using High Temperature Superconducting (HTS) thin films [4–16]. These thin film filters require either sputtered thin films or the better quality laser ablated thin films. Even though the laser ablated HTS films have the lowest AC losses and provide the best filtering characteristics, they are costly and their production throughputs are very low. The Seeded Melt Grown (SMG) superconductor crystals have relatively low losses compared to the sputtered films and similar losses compared to the laser ablated films [4–16]. On the other hand SMG-HTS bulk material production is comparatively very cheap and these materials can be produced in large quantities with a high throughput.

This paper describes a method to reduce the size of cavity filters by use of re-entrant cavity structures made form SMG-YBCO superconductors. Though the re-entrant structure processed from ordinary conductors is relatively lossy, the results presented here show that, with the use of superconducting material, the cavity losses are reduced dramatically. As a result, much improved filter characteristics are obtained which significantly enhances the selectivity of such a filter.

2. Experimental details and results

In order to verify the feasibility of re-entrant cavities as low frequency filter elements, a conventional metal version was designed, simulated, fabricated and tested. The design was then extended to the SMG-HTS cavities. For both cases, provisions were made such that by replacing the re-entrant post plates by simple plates, the cavities were also tested as simple cylindrical cavities for which exact design formulas apply.

2.1. Metal cavity resonator

A re-entrant metal cavity was designed, machined and experimentally measured [4,5]. A photograph of the machined cavity and associated dimensions of the re-entrant cavity are shown in Fig. 1. The radius of the fabricated brass cavity r_1 was 15 mm and the height h_0 was 10 mm. The radius of the inner post r_0 was 10 mm and height d was 8.5 mm. These dimensions allowed a 1.5 mm gap ($g = h_0 - d$) between the post top and the bottom surface of the cylindrical cavity.

Replacing the post–plate with a flat plate, corresponding simple cylindrical cavity parameters were also measured. For experimental measurements, a

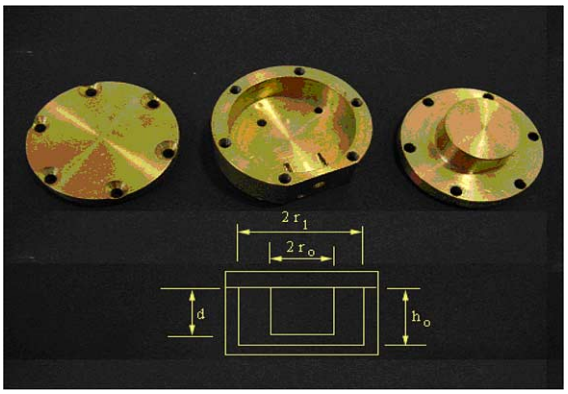

Fig. 1. Machined metal cavity. The flat plate on the left is for conventional cylindrical cavity and the plate on the left with a post is for re-entrant cavity.

single coupling probe was used and it was inserted from the side surface. Care was taken to ensure that the probe tip did not touch the inner post when the re-entrant structure was used.

The simple cylindrical cavity was first simulated in High Frequency Structure Simulator (HFFS) by Ansoft® to determine the pertinent cavity parameters. Fig. 2a shows the simulated transmission characteristic (S_{21}) of the cylindrical metal cavity using two coupling ports. The inset in the same figure shows the simulated structure with the simulated *E*-field distribution within the cavity. Fig. 2b shows the corresponding experimentally measured S_{11}-parameter using only a single coupling port. All these and subsequent experimental data were taken using Agilent-8510C Vector Network Analyser (VNA).

The simulations resulted in the resonant frequency, f_0, of 11.9 GHz and the quality factor, Q, of 7355. The experimental values resulted in a resonant frequency value of 12.15 GHz and Q factor of 6927. Both the simulated and experimentally measured results are listed in Table 1. The experimental measurements for the simple cavity matched quite closely with the results from the simulations. Slight variations in the resonance frequencies between the simulated and measured data may be attributed to the differences in the number of ports, and cavity perturbation due to the presence of the input probe. Also, in the

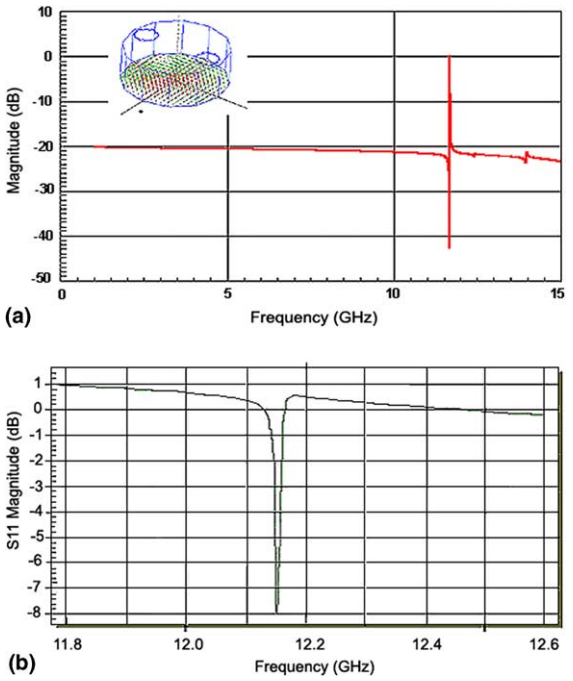

Fig. 2. (a) HFFS simulation for the simple cylindrical metal cavity. Inset shows the simulated structure and surface current distribution. (b) Experimentally measured *S*-parameters for the simple metal cavity.

Table 1
Summary of parameters of re-entrant cavities

Cavity types	Cut-off freq. (GHz)		Q (simulated)	Q (measured)	
	Simulated	Measured		Room T	80 K
Metal cylindrical (TM_{010})	11.9	12.15	7355	6927	
Complete metal re-entrant	3.4	3.48	2586	2103	
Metal + HTS post		4.42		1826	4528
HTS cylinder (TM_{010})	10.6	9.78		1263	2458
HTS complete re-entrant		3.185		2617	6388

simulations, the ports were approximated by conditions that may differ from the actual experimental conditions.

2.2. Re-entrant metal cavity resonator

Replacing the top flat plate with the plate and post combination, the re-entrant metal cavity was simulated and experimentally measured. Fig. 3a shows the simulated S_{21} and Fig. 3b shows the experimentally measured S_{11} of the re-entrant metal cavity. The results are tabulated in Table 1. As expected, both simulated and experimental results show the dramatic decrease of the resonant frequency of a cylindrical structure having the same outer radius r_1 by the insertion of a central post to form the re-entrant cavity. Measured resonant frequency of 12.15 GHz for the cylindrical cavity decreased to 3.48 GHz for this geometry. These simulations and experimental results verify the concept of using a re-entrant cavity as filter elements.

As expected, re-entrant cavity performance using conventional metal cavities showed that the resonator structure was relatively lossy. To overcome these disadvantages, the replacement of the whole re-entrant cavity structure by a high T_c superconducting material was explored. High temperature superconducting materials such as $YBa_2Cu_3O_x$ (YBCO) offer promise in this regard by virtue of their extremely low surface resistance at cellular frequencies [17–23]. Recent developments in the controlled growth of single-domain YBCO, however, offers an alternative technique for fabricating HTS components in a variety of shapes, and particularly in making compact, light weight, and tunable high frequency components and devices for wireless telecommunications and other electronic applications.

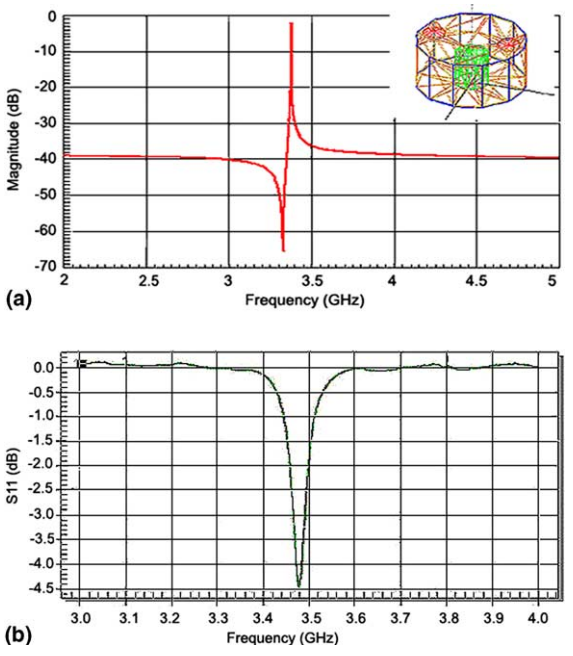

Fig. 3. (a) HFFS simulation for the re-entrant metal cavity. Inset shows the simulated structure. (b) Experimentally measured *S*-parameters for the re-entrant metal cavity.

2.3. Crystal growth of the YBCO superconductor

The Seeded Melt Growth (SMG) method for processing bulk superconductors was originally developed to produce large domain HTS materials for levitation applications [17–19]. The SMG process is based on the concept of crystal growth, in which a small "seed" crystal with a higher melting point (compared to that of the precursor compound) is placed on the surface of the partially molten precursor pellet. Initial growth of the sample then takes place at the interface between the seed surface and the liquid during cooling. In addition, the growth assumes the orientation of the seed and eventually proceeds throughout the entire precursor pellet. In this way, large single-crystal-like domain materials can be obtained.

Precursor powders of 70 wt.% $YBa_2Cu_3O_x$, 30 wt.% Y_2BaCuO_5, and 0.15 wt.% Pt were mixed thoroughly and pressed uniaxially at 100 MPa into a disc-shaped green pellet. The green pellet was sintered in air at 930 °C for 24 h to form a solid ceramic body. A $SmBa_2Cu_3O_x$ single domain of dimensions $2 \times 2 \times 1.5\ mm^3$ was used as seed crystal. Prior to grain growth, the seed was placed on the top surface of the green pellet at room temperature. The pellet and seed crystal was then placed on an alumina plate with an intermediate layer of Y_2O_3 powder to avoid liquid loss to the interior surfaces of the furnace at elevated temperature. A sintered thin plate of a mixture of $YbBa_2Cu_3O_x$ and $YBa_2Cu_3O_x$ was also used between the green

pellet and the Y_2O_3 layer. Full details of the YBCO single domain growth process can be found in Refs. [17–24].

In order to use the single domain YBCO for high performance microwave communication components, a cylindrical cavity resonator was designed with a flat plate closed end, as shown in Fig. 4. For this design, a novel net-shape process was developed based on the conventional SMG approach, which was modified as follows: (1) The pellet was pressed and machined into the desired geometry in the green state; (2) The seed was located in the center of inner surface for the optimum growth, and (3) The growth was controlled so that the entire preshaped pellet could grow completely into a single domain. The interior of the single domain cavity was hand-polished down to 1/4 μm with diamond paste. The polished samples were annealed in flowing oxygen at 400 °C for 10 days.

2.4. Cavity filter using YBCO superconductor

Experiments were performed on a cavity resonator made completely of bulk superconductor in order to investigate the suitability of this material for filter applications. In these experiments, a cavity made of YBCO was cooled in a cryogenic chamber and the *S*-parameters of the filter at various temperatures were recorded. Readings were taken at different temperatures during the cooling process using a programmable temperature controller.

Two types of superconducting cavities were investigated experimentally. The first experiment was a conventional cylindrical cavity made from SMG-YBCO. In the second experiment, a plug was introduced into the centre of the top cover of the cavity to form a re-entrant structure. The cylindrical YBCO cavity had a radius r_1 of 11 mm and a height h_0 of 10 mm.

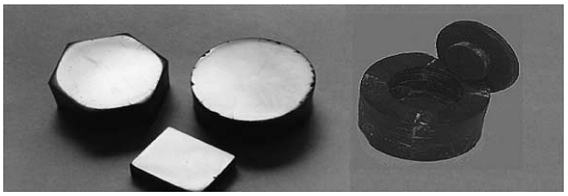

Fig. 4. As-grown YBCO samples and re-entrant cavity.

The performance of the simple HTS cylindrical cavity was also simulated over a wide frequency range to observe the two lowest resonant modes. For this simulation, it was assumed that the cavity walls had infinite conductivity. The simulated results over a wide frequency range are shown in Fig. 5. The lower frequency corresponds to the TM_{010} mode (theoretical resonant frequency $f_0 = 10.44$ GHz) and the higher frequency to the TE_{111} mode of the cavity (theoretical resonant frequency $f_0 = 17.0$ GHz). For the experimental measurements, the VNA was swept around the center frequencies of the corresponding modes predicted by the simulations. Typical VNA input reflection coefficients readings (S_{11} in dB) for the TM_{010} mode at room temperature, at 80 K and 20 K are shown in Fig. 6.

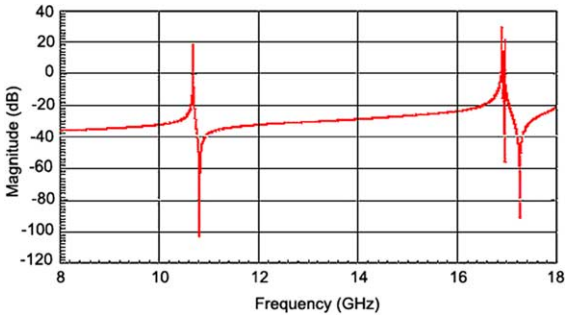

Fig. 5. First and second resonances in the superconducting cylindrical cavity from simulation. The lowest order mode was the TM_{010} mode at 10.6 GHz and the next two higher modes were the TM_{110} and TE_{111} modes close at 17.0 GHz.

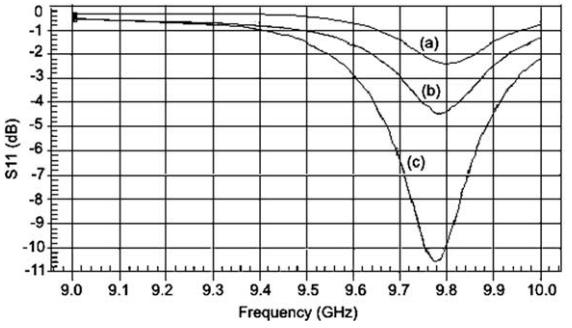

Fig. 6. *S*-parameters of the TM_{010} mode of the superconducting cavity at 9.8 GHz at (a) room temperature, (b) at 80 K and (c) 20 K.

Similar measurements were made within the frequency range of the TE_{111} mode. In both cases, the measured values were slightly lower in frequency than the simulated values due to the insertion of the probes and to slight variations in the dimensions of the cavity. Also two ports were used in the simulations and in the measurements only a single port was used. In both experiments, the temperature was varied over a wide range from room temperature down to 10 K and the Q values were calculated from the measured data. The calculated loaded Q_L and unloaded Q_0 at various temperatures are plotted in Figs. 7 and 8 for the respective TM_{010} and TE_{111} modes. From these graphs, it can be seen that there are significant changes in the Q factors as a function of temperature. There is a distinct and abrupt change in the quality factor at the critical temperature where the material becomes superconducting. The Q values continue to increase as the temperature is further lowered. Since these experiments were to verify the concepts of using SMG-YBCO bulk material as cavity filter elements, in these and in the subsequent experiments, input power dependence on the cavity parameters were not investigated. All these measurements were made using a fixed input signal power level.

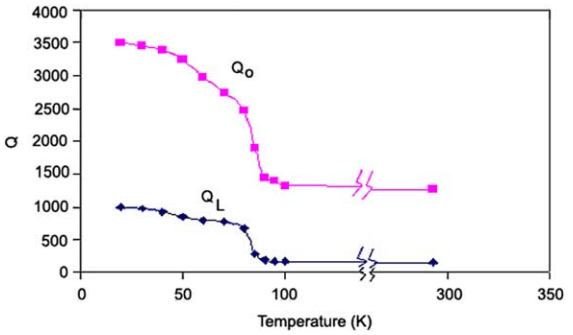

Fig. 7. Unloaded and loaded Q of the superconducting cavity vs. temperature of the TM_{010} mode at 9.8 GHz.

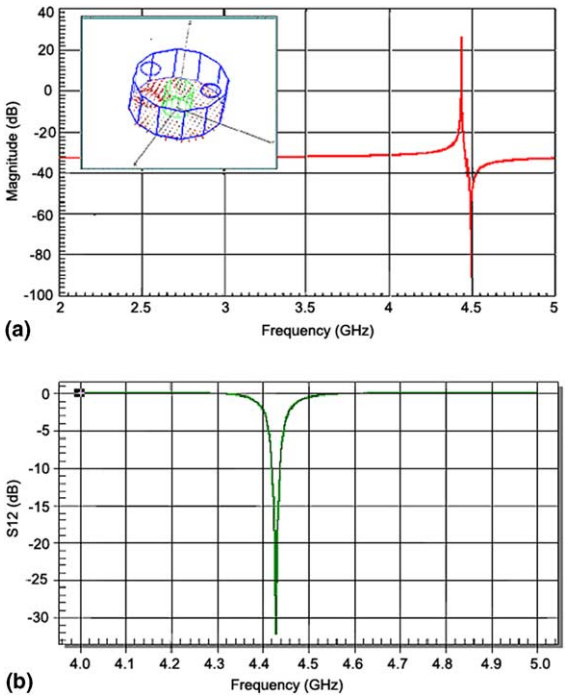

Fig. 8. (a) Simulated S-parameters of the re-entrant metal cavity with superconducting post. The inset shows the simulated E-fields. (b) S-parameters of the re-entrant metal cavity with superconducting post at 80 K.

2.5. Re-entrant cavity using YBCO superconductor

In order to manufacture superconducting re-entrant cavities, either the entire structure can be machined from a single superconducting crystal or just the inner post can be made of superconducting material. In order to demonstrate the feasibility of these concepts, both experiments have been carried out, one using the superconducting material only for the central post in a metal cavity and the other using a complete structure fabricated from YBCO.

2.5.1. Re-entrant cavity with a superconducting cylindrical post

A YBCO single domain re-entrant post was fabricated and the performance of the re-entrant cavity simulated for the measured dimensions of the post. For the main cavity, the metal cylinder detailed in Section 1 was used.

The results of the simulation are given in Fig. 9a. The corresponding measured sample data at 80 K is shown in Fig. 9b. The experimental data show a resonance frequency of 4.42 GHz. Q values are 1826 at room temperature, and 4528 at 80 K, respectively. The resonance becomes sharper in the superconducting state. It is apparent that the

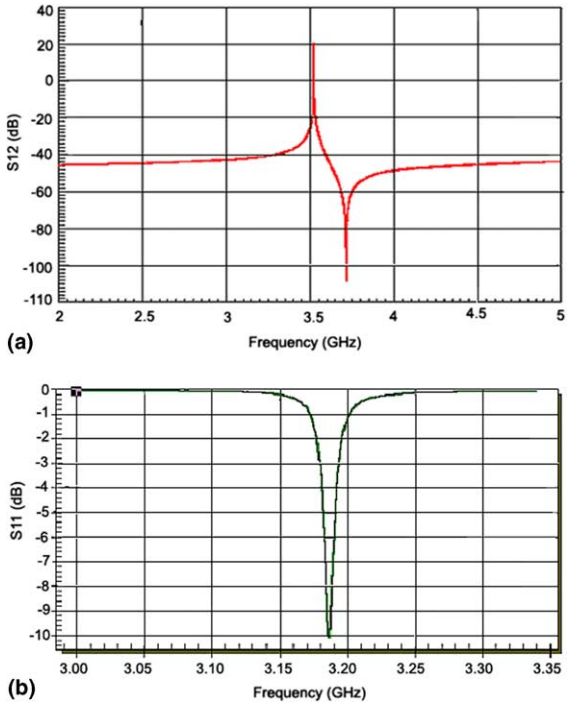

Fig. 9. (a) Simulation results of the completely superconducting re-entrant cavity. (b) S-parameters of the superconducting re-entrant cavity filter with superconductor at a temperature of 80 K.

use of a superconducting re-entrant post has significantly reduced the losses in the structure and increased the Q factor. Compared to the re-entrant cavity with a metal post where the Q_0 was 2103, Q_0 with a superconducting post was almost doubled.

2.5.2. Complete superconducting re-entrant cavity filter

After verifying that the superconducting post in the cavity dramatically improved the filter characteristics, a set of YBCO single domain re-entrant cavities were fabricated and tested to verify that the results for re-entrant cavities were consistent. The new cavity had the following dimensions: outer cavity radius r_1 was 11 mm; height of the cavity h_0 was 10 mm; height of the inner post d was 8.5 mm and post radius r_0 was 7 mm, gap $(h_0 - d)$ again was 1.5 mm, etc.

Fig. 9a shows the simulated HFSS results, assuming infinite conductivity for the cavity walls, while Fig. 9b shows the measured S-parameters at

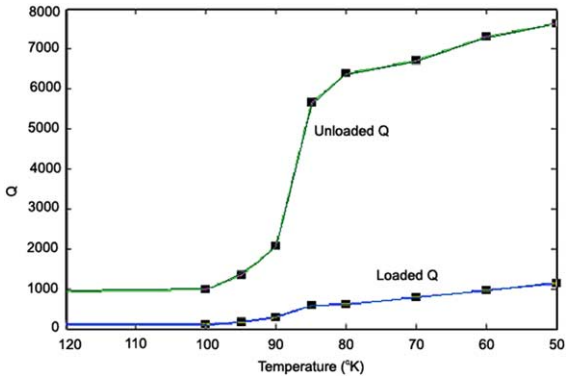

Fig. 10. Unloaded and loaded Q of the superconducting re-entrant cavity at 3.5 GHz.

80 K, respectively. The experiments resulted in a resonant frequency of 3.185 GHz. The Q values were 2617 at room temperature and 6388 at 80 K.

Fig. 10 shows as a function of temperature the variation of loaded and unloaded Q values for the completely superconducting re-entrant cavity. The simulated and experimental results for various re-entrant cavities are summarized in Table 1. It should be noted that the dimensions of the metal and HTS cylindrical cavities are not the same.

In all these experiments, it was shown that the re-entrant cavity resonator processed completely from superconducting material had a highest quality factor. From our earlier measurements, the surface resistance R_s of the SMG grown YBCO has a very low surface resistance comparable to that of the laser sputtered YBCO thin films [25]. When these values were used to calculate the theoretical Q values for cylindrical superconducting cavities, measured Q values were always lower than the calculated values.

The lower Q values for the superconducting cavities can be attributed to two major factors. The first factor can be attributed to the crystalline structure of the YBCO crystal. The R_s measurements previously made were on the polished surface of the crystalline YBCO which was perpendicular to the c-axis of the crystal. On the other hand, when a cylindrical cavity was processed using the novel net-shape process, the inner cylindrical surfaces of the cavities were only polished. These surfaces are parallel to the c-axis of the crystal. AC losses on these surface properties

may be larger than the surfaces that are perpendicular to the c-axis. At present, these surface qualities are being investigated in detail.

The second factor is that the cover top plate of the cavity was held in place by mechanical compression. Small gaps between the top surfaces of the cylinder and the cover plate may provide breaks in the continuity of the cavity surface currents. These breaks will increase the associated losses and thus further reduce the measured Q values. This can easily be remedied by joining the top plate to the cylinder by YBCO paste and by post sintering.

3. Conclusions

In this study, we have demonstrated the feasibility of using a re-entrant cavity structure for reducing the bulky size of the cavity filters. We have also shown that with the use of a superconducting material, the filter characteristics can be greatly improved and a filter with an extremely high selectivity can be achieved. As a result, we have simulated a wideband filter using multiple coupled re-entrant cavity structures. This work will be presented once the necessary measurements are completed.

The immediate practical utility of HTS devices in high frequency filter applications is currently limited by the availability of low cost cryogenic coolers required to cool the material to the superconducting state. However, even with these constraints, it is anticipated that the use of HTS filters will be required in the near future as urban wireless markets become more and more overcrowded. Therefore, the improved filter characteristics of the re-entrant filter structure investigated in this present study, coupled with the advantage of the lower cost bulk SMG superconductors, will certainly find valuable commercial applications in this ever increasing wireless age.

References

[1] C.W. Sayre, Complete Wireless Design, McGraw-Hill, 2001.
[2] D.M. Pozar, Microwave Engineering, John Wiley & Sons, 1998.
[3] S.C. Harsany, Principles of Microwave Technology, Prentice Hall, 1997.
[4] H. Pandit, High T_c superconductor re-entrant cavity filter structures, Masters Thesis, University of Cincinnati, 2003.
[5] R.S. Kwok, J.-F. Liang, IEEE Trans. MTT 47 (1) (1999).
[6] J.E. Aitken, Swept-Frequency Microwave Q-Factor Measurement, 1976.
[7] T. Koru Ishii, Microwave Engineering, International Thomson Publications, 1997.
[8] C. Wang, H.-W. Yao, K.A. Zaki, in: IEEE Antennas and Propagation Society Symposium, July 1996, vol. 1, p. 280.
[9] B.D. Zhang et al., IEEE Trans. Appl. Supercond. 5 (1995) 2656.
[10] D. Dijkkamp, T. Venkatesan, X.D. Wu, S.A. Shaheen, N. Jisrawi, Y.H. Min-Lee, W.L. McLean, M. Croft, Appl. Phys. Lett. 51 (1987) 619.
[11] T. Koru Ishii, Microwave Engineering, Hartcourt Bracejovanovich, 1989.
[12] K. Fujisawa, IRE Trans. MTT-6 (1958) 344.
[13] H.C. Li, G. Linger, F. Ratzel, R. Smithey, J. Greerk, Appl. Phys. Lett. 52 (1988) 1098.
[14] R.L. Sandstrom, W.J. Gallagher, T.R. Dinger, R.H. Koch, Appl. Phys. Lett. 53 (1988) 444.
[15] C.B. Eom, J.Z. Sun, K. Yamamoto, A.F. Marshall, K.E. Luther, S.S. Laderman, T.H. Geballe, Appl. Phys. Lett. 55 (1989) 595.
[16] R. Wordenweber, J. Einfeld, R. Kutzner, A.G. Zaitsev, M.A. Hein, T. Kaiser, G. Muller, IEEE Trans. Appl. Supercond. 9 (1999) 2486.
[17] D. Shi, W. Zhong, U. Welp, S. Sengupta, V. Todt, G.W. Crabtree, S. Dorris, U. Balachandran, IEEE Trans. Magnet. 5 (1994) 1627.
[18] D. Shi, K. Lahiri, S. Sagar, D. Qu, V. Pan, V.F. Solovjov, J.R. Hull, J. Mater. Res. 12 (1997).
[19] D. Shi, K. Lahiri, J.R. Hull, D. LeBlanc, M.A.R. LeBlanc, A. Dabkowski, Y. Chang, Y. Jiang, Z. Zhang, H. Fan, Physica C 246 (1995) 253.
[20] P. Gautie-Picard, X. Chaud, E. Beaugnon, A. Erraud, R. Tounier, Mater. Sci. Eng. B 53 (1998) 66.
[21] P. Cautier-Picard, E. Beaugnon, X. Chaud, A. Sulpice, R. Torunier, Physica C 308 (1998) 161.
[22] P. Bautier-Picard, E. Beaugnon, R. Tournier, Physica C 276 (1997) 35.
[23] D. Shi, P. Odier, A. Sulpice, D. Isfort, X. Chaud, R. Tournier, P. He, R. Singh, Physica C 384 (2003) 149.
[24] D. Qu, D. Shi, S.L. Lu, A.M. Ferendeci, D. Mast, Physica C 315 (1999) 36.
[25] H. Pandit, A. Mishra, N. Hari Babu, P. He, D. Isfort, X. Chaud, A.M. Ferendeci, D.A. Cardwell, R. Tournier, D. Mast, D. Shi, Physica C 402 (2004) 277.